

# Orai1 and STIM1 Are Critical for Breast Tumor Cell Migration and Metastasis

Shengyu Yang,<sup>1</sup> J. Jillian Zhang,<sup>1</sup> and Xin-Yun Huang<sup>1,\*</sup>

<sup>1</sup>Department of Physiology, Weill Medical College of Cornell University, New York, NY 10065, USA

\*Correspondence: xyhuang@med.cornell.edu

DOI 10.1016/j.ccr.2008.12.019

## SUMMARY

Tumor metastasis is the primary cause of death of cancer patients. Understanding the molecular mechanisms underlying tumor metastasis will provide potential drug targets. We report here that Orai1 and STIM1, both of which are involved in store-operated calcium entry, are essential for breast tumor cell migration in vitro and tumor metastasis in mice. Reduction of Orai1 or STIM1 by RNA interference in highly metastatic human breast cancer cells or treatment with a pharmacological inhibitor of store-operated calcium channels decreased tumor metastasis in animal models. Our data demonstrate a role for Orai1 and STIM1 in tumor metastasis and suggest store-operated calcium entry channels as potential cancer therapeutic targets.

## INTRODUCTION

Despite the significant improvement in both diagnostic and therapeutic modalities for the treatment of cancer patients, metastasis still represents the major cause of mortality, being responsible for ~90% of all cancer deaths (Christofori, 2006; Hanahan and Weinberg, 2000). Metastasis is the multistep process wherein a primary tumor spreads from its initial site to secondary tissues/organs (Fidler, 2003; Weiss, 2000). To disseminate from primary tumors and establish secondary tumors, cancer cells must succeed in migration/invasion, infiltration into circulation, survival in the circulation, penetrating through capillary endothelia, and proliferating to form secondary tumors in distant organs. Failure at any of these steps can block the entire metastatic process. Since tumor spreading is responsible for the majority of deaths of cancer patients, development of therapeutic agents that inhibit tumor metastasis is highly desirable. Such agents could be effective in restraining new tumor formation when earlier therapy or surgery has failed, or in increasing successful containment of solid tumors in combination therapy with other agents. To achieve the goal of preventing tumor metastasis, a better understanding of the molecular components involved in tumor metastasis is needed.

One of the critical steps during tumor metastasis is tumor cell migration and invasion, which are responsible for the entry of

tumor cells into lymphatic and blood vessels as well as the extravasation of tumor cells into the secondary organs (Mareel and Leroy, 2003; Steeg, 2006). Cell migration is a sequential and interrelated multistep process involving the formation of lamellipodia/membrane protrusions at the front edge, cycles of adhesion and detachment, cell body contraction, and tail retraction (Ridley et al., 2003). Focal adhesion turnover plays a pivotal role in cell migration. Small, nascent focal adhesions at the leading edge serve as traction points for the forces that move the cell body forward. On the other hand, disassembly of focal adhesions at the rear allows the retraction of the rear and net translocation of the cell in the direction of movement (Webb et al., 2002). To extravasate through capillary endothelium, cancer cells need to adhere to endothelial cells. During migration and invasion, the adhesions between cancer cells and the extracellular matrix also undergo disassembly (Webb et al., 2002). Recently, ~20% of the cancer candidate genes in breast and colorectal cancers were found to be adhesion-related genes, implying the significance of cell adhesion in cancer progression (Sjoblom et al., 2006).

The ubiquitous second messenger  $\text{Ca}^{2+}$  is one of the critical regulators of cell migration (Pettit and Fay, 1998). We and others have previously shown that  $\text{Ca}^{2+}$  influx is essential for the migration of various cell types, including tumor cells (Komuro and Rakic, 1993; Lee et al., 1999; Marks and Maxfield, 1990; Nishiyama et al.,

## SIGNIFICANCE

The primary cause of death of cancer patients is tumor metastasis, that is, the spreading of tumors from the primary site to secondary sites. Thus, development of drugs targeting this spreading process is desirable. Cell migration is one of the key steps in tumor spreading. Therefore, it is likely that inhibitors of cell migration can block tumor metastasis. The proteins Orai1 and STIM1 have recently been identified to be involved in calcium influx from the extracellular environment to the inside of cells. We show here that Orai1 and STIM1 are required for tumor cell migration, invasion, and metastasis. Hence, Orai1 and STIM1 are potential targets for therapeutic intervention to inhibit tumor metastasis.

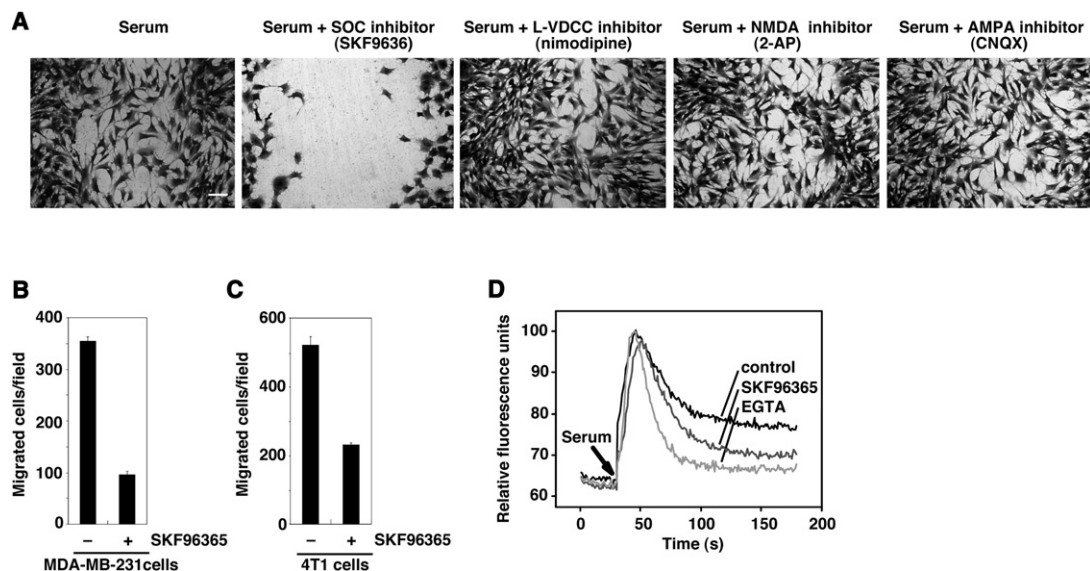


**Figure 1.  $\text{Ca}^{2+}$  Influx Is Required for Serum-Induced Cell Migration**

(A) Wound-healing assays showing that SKF96365 (20  $\mu\text{M}$ ) inhibits the migration of MEFs. Nimodipine (20  $\mu\text{M}$ ), DL-2-amino-5-phosphonopentanoic acid (2-AP) (1 mM), and CNQX (10  $\mu\text{M}$ ) had no effect on MEF migration. Scale bar = 100  $\mu\text{m}$ .

(B) Boyden chamber assay showing that SKF96365 (10  $\mu\text{M}$ ) decreases serum-induced migration of MDA-MB-231 human breast tumor cells.

(C) Boyden chamber assay showing that SKF96365 (10  $\mu\text{M}$ ) decreases the migration of 4T1 mouse mammary tumor cells induced by serum.

(D) Fluo-3  $\text{Ca}^{2+}$  imaging indicates that SKF96365 (10  $\mu\text{M}$ ) and EGTA (2 mM) treatments decrease serum-induced  $\text{Ca}^{2+}$  influx in MEFs.

Data are either representative of three similar experiments or are shown as mean  $\pm$  SD of five experiments.

2003; Yang and Huang, 2005). In nonexcitable cells, store-operated calcium influx is the predominant  $\text{Ca}^{2+}$  entry mechanism (Lewis, 2007; Parekh and Penner, 1997). Recent studies have identified two genes, *STIM1* (stromal interaction molecule 1) and *Orai1* (also named *CRACM1*), that are responsible for store-operated  $\text{Ca}^{2+}$  entry (Feske et al., 2006; Liou et al., 2005; Roos et al., 2005; Vig et al., 2006; Zhang et al., 2006). While *STIM1* serves as a  $\text{Ca}^{2+}$  sensor, *Orai1* is an essential pore-forming component of the store-operated  $\text{Ca}^{2+}$  entry channel (Prakriya et al., 2006; Yeromin et al., 2006). Coexpression of *Orai1* and *STIM1* is sufficient to reconstitute the store-operated calcium channel function (Mercer et al., 2006; Peinelt et al., 2006; Soboloff et al., 2006). Store-operated calcium influx controls a variety of physiological and pathological processes (Dolmetsch et al., 1998; Fanger et al., 1995; Feske et al., 2005; Lewis, 2001; Mogami et al., 1997; Yoo et al., 2000). However, the roles of store-operated calcium influx in tumor metastasis have not been investigated. Here we examined the role of *Orai1* and *STIM1* in breast tumor cell migration, invasion, and metastasis.

## RESULTS AND DISCUSSION

### Store-Operated $\text{Ca}^{2+}$ Channels Are Critical for Serum-Induced Cell Migration

We have previously shown that  $\text{Ca}^{2+}$  influx is required for both growth factor- and serum-induced fibroblast cell migration (Yang and Huang, 2005). To understand the molecular mechanisms, we investigated the effect on cell migration of pharmacological inhibitors for various ion channels that mediate  $\text{Ca}^{2+}$  influx (Figure 1A). While inhibitors of voltage-gated  $\text{Ca}^{2+}$  channels (nimodipine), NMDA receptors (2-AP), or AMPA receptors (CNQX) had no effect

on serum-induced fibroblast cell migration, an inhibitor of store-operated  $\text{Ca}^{2+}$  entry (SKF96365) blocked serum-induced cell migration (Figure 1A). In these wound-healing assays, fibroblasts were grown to confluency, and a "wound" was made in the middle of the tissue culture plate with a pipette tip. In the presence of serum, cells would migrate and fill the gap after  $\sim 12$  hr (Guo et al., 2007; Shan et al., 2006; Wang et al., 2006; Yang and Huang, 2005) (Figure 1A). The inhibitory effect of SKF96365 on cell migration was confirmed with different types of cells and by a different method of measuring cell migration. Using a Boyden chamber assay (counting cells migrating through a porous membrane), we observed that SKF96365 inhibited the migration of MDA-MB-231 human breast cancer cells and 4T1 mouse mammary tumor cells (Figures 1B and 1C). To confirm that SKF96365 blocked serum-induced  $\text{Ca}^{2+}$  influx, Fluo-3 (a fluorescent  $\text{Ca}^{2+}$  indicator)-based  $\text{Ca}^{2+}$  measurement was performed. Normally, a serum-induced  $\text{Ca}^{2+}$  response consists of two phases, a peak phase contributed by  $\text{Ca}^{2+}$  release from intracellular  $\text{Ca}^{2+}$  stores and a plateau phase contributed by  $\text{Ca}^{2+}$  influx (Berridge et al., 2003). As shown in Figure 1D, SKF96365 decreased the amplitude of the plateau phase of the serum-induced  $\text{Ca}^{2+}$  response without affecting the peak phase. Similar results were observed with EGTA, which chelates extracellular  $\text{Ca}^{2+}$  (Figure 1D). These pharmacological inhibitor data show that blocking  $\text{Ca}^{2+}$  influx inhibits serum-induced migration of different types of cells, including breast tumor cells.

We next employed a different approach to verify the role of store-operated  $\text{Ca}^{2+}$  entry in cell migration. Recent studies have identified *STIM1* and *Orai1*, which are responsible for store-operated  $\text{Ca}^{2+}$  entry (Feske et al., 2006; Liou et al., 2005; Roos et al., 2005; Vig et al., 2006; Zhang et al., 2006). To examine whether *STIM1* and *Orai1* are important molecular components

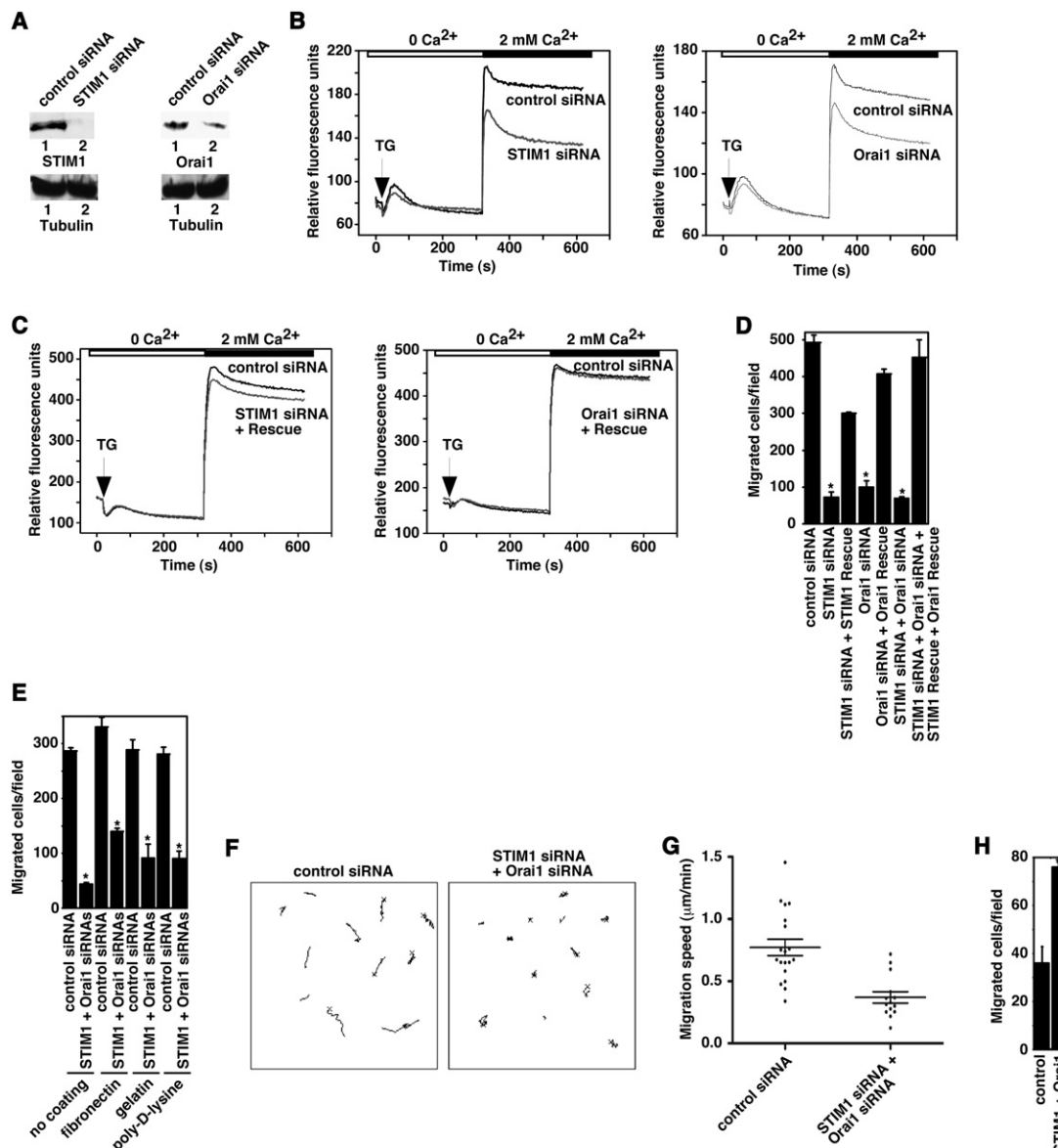


**Figure 2. STIM1 and Orai1 Are Required for Serum-Induced Cell Migration**

(A) Western blots showing that STIM1 siRNA and Orai1 siRNA decrease the protein levels of STIM1 and Orai1, respectively, in MDA-MB-231 cells. One hundred micrograms of total cellular protein was loaded onto each lane.

(B) Fluo-3  $\text{Ca}^{2+}$  measurement indicates that STIM1 siRNA and Orai1 siRNA decrease store-operated  $\text{Ca}^{2+}$  influx in MDA-MB-231 cells. TG, thapsigargin.

(C) Fluo-3  $\text{Ca}^{2+}$  measurement indicates that siRNA-resistant STIM1 or Orai1 constructs restore  $\text{Ca}^{2+}$  influx in STIM1 or Orai1 siRNA-treated cells, respectively.

(D) STIM1 siRNA and Orai1 siRNA decrease serum-induced migration of MDA-MB-231 cells.

(E) STIM1 siRNA and Orai1 siRNA decrease serum-induced migration of MDA-MB-231 cells in Boyden chamber assays with different coatings (including fibronectin, gelatin, and poly-D-lysine) as well as uncoated chamber filter membranes.

(F) Migrating traces, obtained by tracking the movement of cells over the course of 2 hr, of MDA-MB-231 cells expressing control siRNA or STIM1 and Orai1 siRNAs.

(G) Scattered dot plot of cell migration speed obtained by cell tracking. Nineteen control siRNA-treated cells and fourteen STIM1 and Orai1 siRNA-treated cells were tracked. Horizontal bars represent mean ± SEM ( $p < 2 \times 10^{-5}$ ) as calculated by one-tailed Student's *t* test.

(H) Overexpression of STIM1 and Orai1 in MCF-10A epithelial cells enhances the migration of MCF-10A cells.

Data are either representative of three similar experiments or are shown as mean ± SD of five experiments. \* $p < 0.05$ .

involved in cell migration, we used RNA interference (RNAi) to knock down STIM1 and Orai1 in MDA-MB-231 human breast cancer cells. The successful knockdown of STIM1 or Orai1 mRNA was confirmed by western blots with anti-STIM1 or

anti-Orai1 antibodies (Figure 2A). Furthermore, the reduction of functional store-operated  $\text{Ca}^{2+}$  entry was verified by Fluo-3-based measurements (Figure 2B). Store-operated  $\text{Ca}^{2+}$  channels are activated when internal  $\text{Ca}^{2+}$  stores are empty (Lewis,

2007). Thapsigargin was used to empty the intracellular  $\text{Ca}^{2+}$  stores in the absence of extracellular  $\text{Ca}^{2+}$ .  $\text{Ca}^{2+}$  influx was then measured by addition of 2 mM extracellular  $\text{Ca}^{2+}$ . Both STIM1 and Orai1 siRNAs reduced the level of  $\text{Ca}^{2+}$  influx compared to control siRNA against LacZ (Figure 2B). Re-expression of siRNA-resistant STIM1 or Orai1 constructs (generated by mutating the DNA sequences targeted by siRNAs without changing the amino acid sequences) restored the  $\text{Ca}^{2+}$  influx (Figure 2C). Moreover, as measured by Boyden chamber assay, serum-induced MDA-MB-231 cell migration was significantly reduced by STIM1 or Orai1 siRNA treatments (Figure 2D). Several different coatings (including fibronectin, gelatin, and poly-D-lysine) as well as no-coating of the chamber filter membrane produced similar results; STIM1 and Orai1 siRNAs decreased the migration of MDA-MB-231 cells by 60%–85% (Figure 2E). A second set of siRNAs for STIM1 and Orai1 produced similar results (data not shown). Re-expression of siRNA-resistant STIM1 or Orai1 constructs rescued the serum-induced cell migration (Figure 2D). Live-cell tracking revealed that STIM1 siRNA and Orai1 siRNA treatment decreased the migration speed of MDA-MB-231 cells by ~50% (Figures 2F and 2G). In addition, overexpression of STIM1 and Orai1 in MCF-10A epithelial cells (with lower levels of endogenous STIM1 and Orai1 than in MDA-MB-231 cells) enhanced the migration of MCF-10A cells (Figure 2H). STIM1 and Orai1 siRNA treatments did not affect the proliferation of MDA-MB-231 cells (data not shown). Hence, both pharmacological and RNAi data demonstrate that store-operated  $\text{Ca}^{2+}$  channels are critical for serum-induced cell migration.

### Store-Operated $\text{Ca}^{2+}$ Channels Modulate Focal Adhesion Turnover

To further investigate the mechanism by which  $\text{Ca}^{2+}$  influx controls cell migration, we studied the effect of blocking  $\text{Ca}^{2+}$  influx on several steps of cell migration. We found that blocking  $\text{Ca}^{2+}$  influx impaired the turnover of focal adhesions (Figure 3) but had no effect on lamellipodium formation (data not shown). Focal adhesions are the cell adhesions mediated by interaction of integrin with the extracellular matrix (Guo and Giancotti, 2004; Webb et al., 2002). Assembly and disassembly of focal adhesions are required for cell migration (Webb et al., 2002). Newly assembled focal adhesions at the protrusion front of migrating cells provide anchorage points for the actin meshwork to generate traction forces that move the cell body forward, while disassembly of focal adhesions in the back is necessary for the retraction of the trailing tail. Focal adhesions can be visualized by immunostaining for vinculin, a major component of focal adhesions. Murine embryonic fibroblasts (MEFs) plated on gelatin-coated glass coverslips were treated with serum with or without pharmacological inhibitors for 2 hr, fixed with 3.7% formaldehyde, and then stained with vinculin antibody. In control cells, vinculin staining showed a punctate pattern of small focal adhesions, typical of fibroblasts (Figure 3A). Chelation of extracellular  $\text{Ca}^{2+}$  with EGTA induced large peripheral adhesions while decreasing the number of adhesions in the middle of the cell (Figures 3A and 3B). Similarly, treatment of fibroblasts with SKF96365 increased the size of focal adhesions around the periphery of the cells (Figures 3A and 3B). Large peripheral focal adhesions were observed in 74%  $\pm$  5.7% of cells treated with EGTA ( $n = 110$ ), 77%  $\pm$  8.4% of cells treated with  $\text{Ni}^{2+}$  (another  $\text{Ca}^{2+}$  influx

blocker) ( $n = 179$ ), and 86%  $\pm$  3.5% of cells treated with SKF96365 ( $n = 150$ ), but in only ~10% of control cells ( $n = 231$ ) (Figure 3B). On the other hand, treatment of fibroblasts with inhibitors of L-type  $\text{Ca}^{2+}$  channels (nimodipine), NMDA receptors (2-AP), or AMPA receptors (CNQX) did not affect the size of focal adhesions (Figure 3A). Next, to confirm these observations with a different cell type and a different approach, we investigated focal adhesions in MDA-MB-231 human breast tumor cells treated with STIM1 and Orai1 siRNAs (Figure 3C). While focal adhesions were small in control siRNA-treated MDA-MB-231 cells, STIM1 and Orai1 siRNA-treated cells displayed larger peripheral focal adhesions (Figure 3C, upper panels with higher magnification). Re-expression of siRNA-resistant STIM1 or Orai1 constructs reduced the size of focal adhesions to those observed in control siRNA-treated cells (Figure 3C). Quantitative analyses of focal adhesions showed that both the relative integrated intensity and the area of focal adhesions were increased by treatment with STIM1 or Orai1 siRNAs (Figures 3D and 3E). Compared to control siRNA-treated cells, the size of focal adhesions in STIM1 or Orai1 siRNA-treated cells was 3-fold larger and the intensity was 7-fold greater. These increases were prevented by the reintroduction of siRNA-resistant STIM1 or Orai1 constructs (Figures 3D and 3E). Since large peripheral focal adhesions are often correlated with turnover defects, these data indicate that store-operated  $\text{Ca}^{2+}$  channels may regulate cell migration at least partly through modulating focal adhesion turnover.

Since focal adhesion turnover includes focal adhesion assembly (formation of focal complexes) and focal adhesion disassembly, we used live-cell imaging to quantify the rates of focal adhesion assembly and disassembly (Figures 4A–4D; see also Movies S1 and S2 available online). To monitor the dynamic turnover of focal adhesions, we transfected paxillin-GFP into fibroblasts. Paxillin is another major component of focal adhesions. From the live-cell time-lapse recordings, we observed that SKF96365 treatment prevented formation of new focal complexes at cell protrusions and also slowed the disassembly of focal adhesions. In control cells, focal adhesions assembled at a rate of 0.22/min and disassembled at a rate of 0.21/min, consistent with previous reports (Webb et al., 2004) (Figures 4A, 4C, and 4D). In contrast, formation of new focal complexes and disassembly of focal adhesions in SKF96365-treated cells were delayed, with an assembly rate of 0.046/min and a disassembly rate of 0.021/min (Figures 4B–4D). Moreover, nascent focal adhesions generally accompanied the formation of new membrane protrusions in control cells, while nascent adhesions were usually absent from new protrusions in SKF96365-treated cells. Consequently, when migrating cells were treated with SKF96365, new protrusions failed to attach to the substratum and thus quickly withdrew (Movies S1 and S2). Hence, blocking  $\text{Ca}^{2+}$  influx affects both the assembly and disassembly of focal adhesions, which may impair traction force generation in migrating cells.

### The Small GTPases Ras and Rac Can Rescue the Defects of Focal Adhesion Turnover and Cell Migration Induced by Blocking $\text{Ca}^{2+}$ Influx

To further understand the mechanism by which  $\text{Ca}^{2+}$  influx regulates focal adhesion turnover, we investigated the participation of small GTPases, since Ras and Rac are regulators of focal



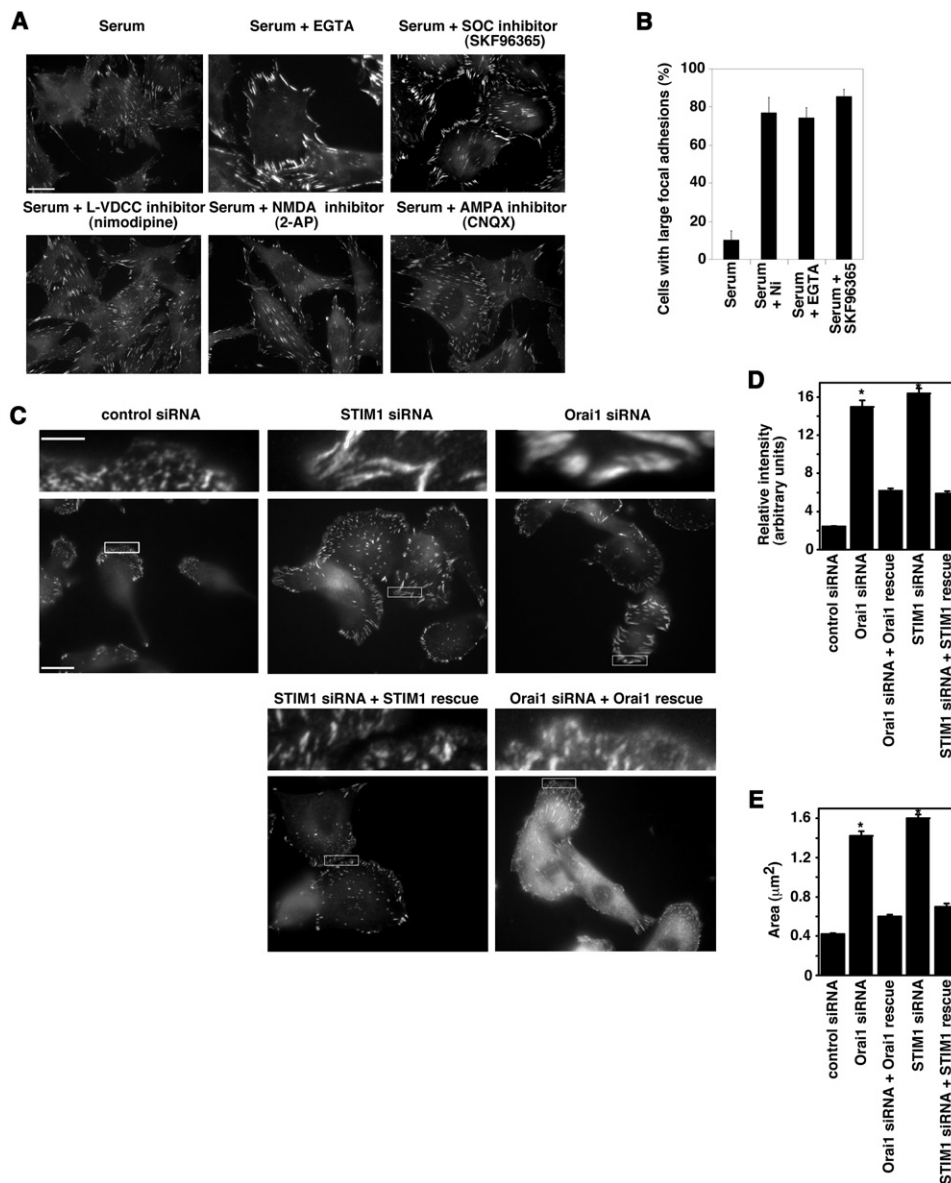


**Figure 3. Blocking  $\text{Ca}^{2+}$  Influx Impairs Focal Adhesion Turnover**

(A) Vinculin staining of fibroblasts. Treatment with EGTA (2 mM) or SKF96365 (20  $\mu\text{M}$ ) induced large peripheral focal adhesions in MEFs. Nimodipine (20  $\mu\text{M}$ ), 2-AP (1 mM), or CNQX (10  $\mu\text{M}$ ) had no effect. SOC: store-operated  $\text{Ca}^{2+}$  entry channel. Scale bar = 10  $\mu\text{m}$ .

(B) Quantification of cells with large peripheral focal adhesions. 1 mM  $\text{Ni}^{2+}$ , 2 mM EGTA, or 20  $\mu\text{M}$  SKF96365 was used for blocking  $\text{Ca}^{2+}$  influx. Data are shown as mean  $\pm$  SD of three experiments.

(C) Vinculin staining of MDA-MB-231 cells. STIM1 siRNA and Orai1 siRNA induced large peripheral focal adhesions in MDA-MB-231 cells. A magnified view of the respective boxed area is shown above each main image. Scale bar = 20  $\mu\text{m}$  for main images and 4  $\mu\text{m}$  for magnified images.

(D and E) Quantification of focal adhesions. The relative integrated intensity (D) and the area (E) of focal adhesions under different conditions were quantified. Data are expressed as mean  $\pm$  SEM of 600–1000 focal adhesions in 10–15 cells and were quantified for each type of cell. \* $p < 10^{-5}$ .

adhesion turnover (Ridley and Hall, 1992; Schlaepfer and Hunter, 1998). We treated cells with the  $\text{Ca}^{2+}$  influx inhibitor SKF96365, and this treatment induced large focal adhesions due to the defective focal adhesion turnover (red vinculin staining in Figure 4E). Expression of constitutively active Ras(G12V) rescued this defect and led to smaller focal complexes (green-labeled cells in Figure 4E). Similarly, constitutively active Rac1(G12V) rescued the SKF96365 effect on focal adhesion turnover (Fig-

ure 4F). Furthermore, dominant-negative Ras and Rac1 mutants induced the formation of larger focal adhesions in MDA-MB-231 cells, implying that these small GTPases are required for focal adhesion turnover (data not shown). Moreover, these rescue effects could be extended to cell migration. While Orai1 and STIM1 siRNA treatment decreased the migration of MDA-MB-231 cells, expression of constitutively active Ras(G12V) rescued the migration of these siRNA-treated cells (Figure 4G).

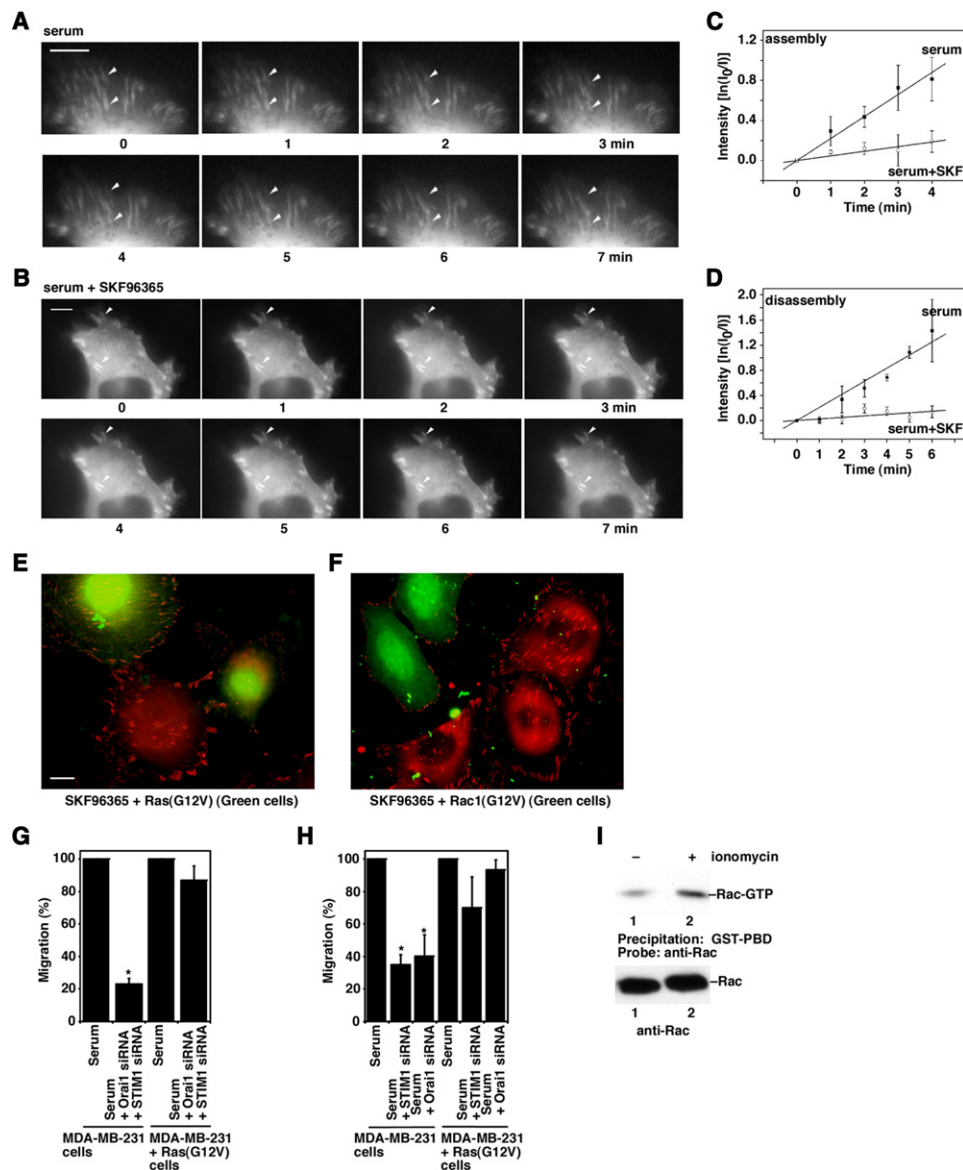


**Figure 4. Blocking  $\text{Ca}^{2+}$  Influx Impairs the Assembly and Disassembly of Focal Adhesions**

(A and B) Live-cell imaging of paxillin-GFP-transfected MEFs in the absence (A) or presence (B) of SKF96365. Scale bar = 10  $\mu\text{m}$ .

(C and D) Quantification of assembly (C) and disassembly (D) of focal adhesions from live-cell time-lapse recordings of paxillin-GFP-transfected cells.

(E and F) MEFs were infected with the retroviruses pBMN-H-Ras(G12V)-IRES-GFP (E) or pBMN-Rac1(G12V)-IRES-GFP (F). These cells were then treated with 10  $\mu\text{M}$  SKF96365 for 2 hr and stained with anti-vinculin antibody. Red indicates vinculin staining; green indicates GFP. Scale bar = 10  $\mu\text{m}$ .

(G and H) MDA-MB-231 cells were infected with the retroviruses pBMN-H-Ras(G12V)-IRES-GFP (G) or pBMN-Rac1(G12V)-IRES-GFP (H). Some of these cells were then treated with Orai1 and/or STIM1 siRNAs. Cells were then used for Boyden chamber assay.

(I) Activation of Rac by  $\text{Ca}^{2+}$  influx. Active Rac (Rac-GTP) proteins were precipitated with the Rac-binding domain of PAK (GST-PBD). Western blots were performed with anti-Rac antibody. Lane 1, starved MDA-MB-231 cells; lane 2, starved MDA-MB-231 cells treated with 500 nM ionomycin for 30 min.

Data are representative of three similar experiments or are shown as mean  $\pm$  SD of three experiments. \* $p < 0.05$ .

Constitutively active Rac1(G12V) also rescued the migration defect induced by Orai1 siRNA or STIM1 siRNA treatments (Figure 4H). In addition,  $\text{Ca}^{2+}$  influx (induced by ionomycin treatment) activated Rac by  $\sim 2$ -fold in MDA-MB-231 cells (Figure 4I). These data suggest that the small GTPases Ras and Rac can rescue the defects of focal adhesion turnover and cell migration induced by blocking  $\text{Ca}^{2+}$  influx.

### Orai1 and STIM1 siRNAs Inhibit Human Breast Tumor Metastasis in a Mouse Model

During the multistep process of tumor metastasis, tumor cell migration and invasion are critical (Mareel and Leroy, 2003; Steeg, 2006). We first investigated the role of STIM1 and Orai1 in tumor cell invasion. Control siRNA-, STIM1 siRNA-, or Orai1 siRNA-treated MDA-MB-231 human breast tumor cells were

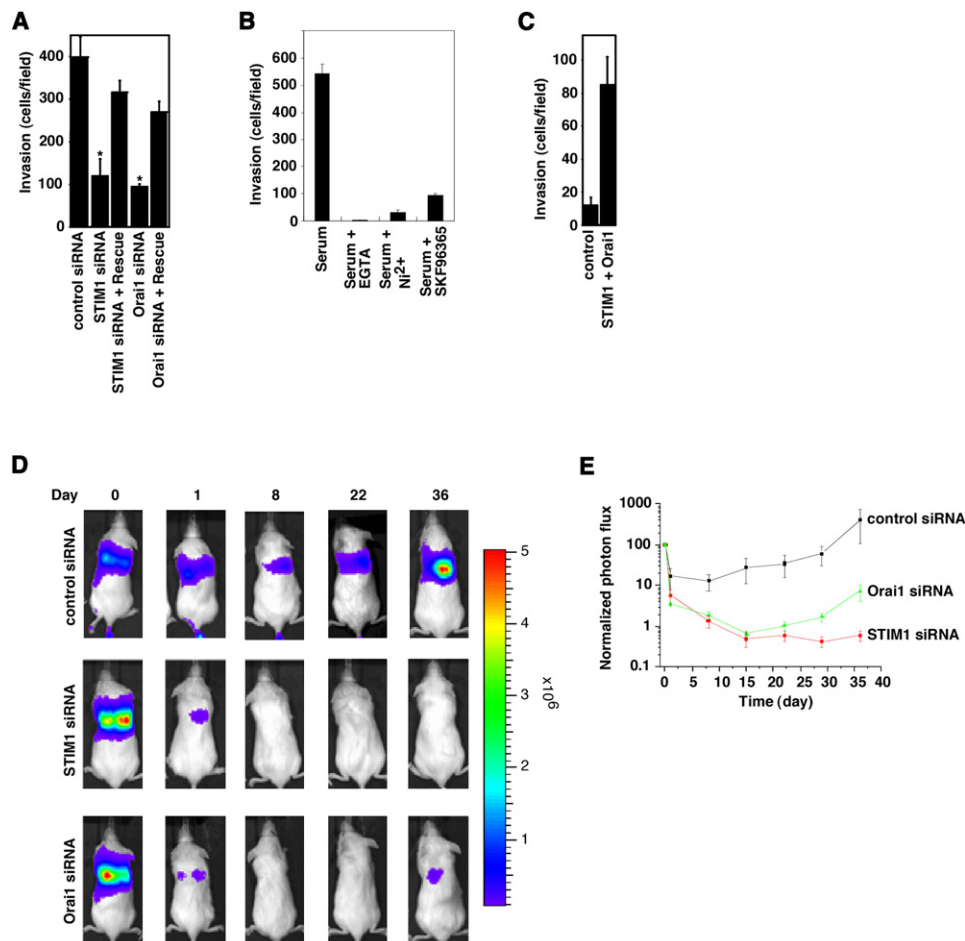


**Figure 5. STIM1 and Orai1 Are Critical for Tumor Cell Invasion and Metastasis**

(A) STIM1 siRNA and Orai1 siRNA treatments decrease the invasion of MDA-MB-231 cells. \* $p < 0.05$ .

(B) EGTA (2 mM), Ni<sup>2+</sup> (1 mM), and SKF96365 (20  $\mu$ M) decrease the invasion of MDA-MB-231 cells.

(C) Overexpression of STIM1 and Orai1 in MCF-10A epithelial cells enhances invasion.

(D) Representative bioluminescent imaging of mice injected with MDA-MB-231 cells stably expressing control siRNA ( $n = 7$ ), STIM1 siRNA ( $n = 9$ ), or Orai1 siRNA ( $n = 8$ ). The photon flux scale is shown at the right.

(E) Quantification of bioluminescent imaging data.

Data in (A)–(C) are shown as mean  $\pm$  SD of three experiments; data in (D) are representative of seven, nine, or eight similar experiments; and data in (E) are shown as mean  $\pm$  SD of seven, eight, or nine experiments.

allowed to migrate through Matrigel. As shown in Figure 5A, fewer STIM1 or Orai1 siRNA-treated MDA-MB-231 cells than control siRNA-treated tumor cells invaded the Matrigel. Re-expression of siRNA-resistant STIM1 or Orai1 constructs rescued the invasion of the STIM1 or Orai1 siRNA-treated cells (Figure 5A). Furthermore, blocking Ca<sup>2+</sup> influx with EGTA, Ni<sup>2+</sup>, or SKF96365 similarly decreased the number of MDA-MB-231 tumor cells invading the Matrigel (Figure 5B). Moreover, expression of STIM1 and Orai1 in MCF-10A epithelial cells enhanced the invasion of these cells (Figure 5C). These results suggest that STIM1 and Orai1 are needed for tumor cell invasion.

To extend these studies to an animal model, we studied the metastasis of MDA-MB-231 human breast tumor cells in immunodeficient NOD/SCID mice using a recently developed triple-modality reporter that encodes a fusion protein consisting of thymidine kinase, GFP, and luciferase (Minn et al., 2005a; Pono-

marev et al., 2004). In these xenograft experiments, MDA-MB-231 tumor cells expressing the GFP and luciferase reporter gene were injected into immunodeficient mice through the tail vein (Minn et al., 2005a; Ponomarev et al., 2004). Luciferase-based noninvasive bioluminescence imaging was used to monitor the presence of tumor cells. Most of these tumor cells became trapped in the capillaries of the lungs shortly after injection (due to size restrictions imposed by mouse capillaries, human tumor cells are rarely able to pass from the arterial to the venous system or vice versa by way of the lung; Minn et al., 2005b) (Figure 5D, day 0). A substantial attenuation of bioluminescence signal was observed within the first day, indicating that cells that failed to metastasize were not able to survive (Figures 5D and 5E). Progressively increasing signals after day 8 in mice with control siRNA-treated tumor cells stably expressing siRNA indicated that cells had succeeded in metastasizing and

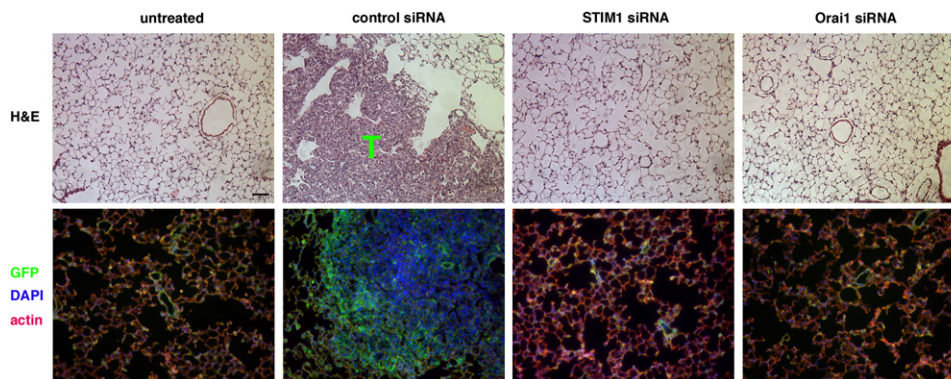


**Figure 6. Blocking  $\text{Ca}^{2+}$  Influx Inhibits Tumor Metastasis**

Histological analyses showing staining of lung tissue sections from untreated mice, mice injected with MDA-MB-231 cells stably expressing control siRNA, mice injected with MDA-MB-231 cells stably expressing STIM1 siRNA, and mice injected with MDA-MB-231 cells stably expressing Orai1 siRNA. The top panels are stained with hematoxylin and eosin (H&E). T indicates tumor metastases. The bottom panels show GFP fluorescence (green), DAPI for nuclei (blue), and rhodamine-conjugated phalloidin for actin polymers (red). Data are representative of three similar experiments. Scale bar = 100  $\mu\text{m}$ .

proliferating (Figures 5D and 5E). Strikingly, the presence of STIM1 or Orai1 siRNA-treated cells stably expressing siRNAs in the lung was much less than control siRNA-treated cells at day 1 and practically undetectable after day 8 (Figures 5D and 5E). Therefore, STIM1 and Orai1 siRNAs significantly inhibit breast tumor metastasis.

To further confirm the defective tumor metastasis, we performed histological analyses of lung tissues from xenografted mice (Figure 6). Tissues were isolated and sectioned, and hematoxylin and eosin (H&E) staining showed normal structure of lungs from noninjected mice (without tumors) and from mice injected with STIM1 or Orai1 siRNA-treated MDA-MB-231 tumor cells (Figure 6). In contrast, lung tissues from mice injected with control siRNA-treated tumor cells were heavily infiltrated by metastasized human breast tumor cells (Figure 6). The identity of tumor cells in the lung tissue was confirmed by GFP fluorescence since the injected MDA-MB-231 tumor cells were labeled with GFP (Figure 6). These results demonstrate that STIM1 and Orai1 are critical for breast tumor metastasis in a mouse model.

#### The Store-Operated Channel Blocker SKF96365 Inhibits Breast Tumor Metastasis in Mouse Models

We further investigated whether the pharmacological inhibitor SKF96365 could be used as a tumor metastasis inhibitor in a mouse model. We first examined lung metastasis of 4T1 mouse mammary tumor cells in mice with or without treatment with SKF96365. The 4T1 mouse tumor closely mimics human breast cancer in its anatomical site, immunogenicity, growth characteristics, and metastatic properties (Pulaski and Ostrand-Rosenberg, 1998; Shan et al., 2005). From the mammary gland, the 4T1 tumor spontaneously metastasizes to a variety of target organs including lung, bone, brain, and liver. Seven days after implantation of 4T1 tumor cells in the mammary glands of BALB/c mice, we injected the mice with control PBS or SKF96365 (daily at 10 mg/kg). After 20 days, the mice were sacrificed and examined for metastasis in the lungs (Shan et al., 2005). Whereas mice injected with control PBS exhibited large numbers of metastasized 4T1 cells in the lungs, the number of

metastasized 4T1 cells in the lungs of mice treated with SKF96365 was reduced by  $\sim 80\%$  (Figure 7A). These results demonstrate that SKF96365 is a potent inhibitor of 4T1 tumor cell metastasis from the mammary gland to the lungs.

The antimetastatic effect of the store-operated channel blocker SKF96365 was next examined in a xenograft mouse model with MDA-MB-231 human breast tumor cells. After tail-vein injection of tumor cells, NOD/SCID mice were intraperitoneally administered 10 mg/kg SKF96365 daily for 4 weeks. The metastasis of tumor cells to the lungs was significantly inhibited after one week of SKF96365 treatment (Figures 7B and 7C). More importantly, even at day 42, two weeks after withdrawal of SKF96365, no increase in metastasis was observed (Figure 7B). Therefore, SKF96365 is an effective inhibitor of breast tumor metastasis in mouse models.

#### Conclusion

We have shown that STIM1 and Orai1 are essential for tumor cell migration in vitro and tumor metastasis in mice. The molecular mechanism by which  $\text{Ca}^{2+}$  influx regulates cell migration at least partly involves the modulation of focal adhesion turnover. Our data demonstrate a role for store-operated  $\text{Ca}^{2+}$  entry in tumor metastasis, making STIM1 and Orai1 attractive targets for therapeutic intervention.

The molecular mechanism by which  $\text{Ca}^{2+}$  regulates focal adhesion turnover is incompletely understood. Focal adhesions are dynamic structures under tight spatial control at the subcellular level to enable localized responses to extracellular cues. Both protein tyrosine phosphorylation and proteolysis of proteins in focal adhesions are involved in focal adhesion turnover (Webb et al., 2002). Increase of cellular  $\text{Ca}^{2+}$  could increase the activity of the tyrosine kinase FAK (focal adhesion kinase) and the calcium-dependent protease calpain in focal adhesions (Achison et al., 2001; Dourdin et al., 2001; Huttenlocher et al., 1997; Siciliano et al., 1996). FAK is a critical regulator of focal adhesion turnover. In FAK-deficient fibroblasts, decreased migration is accompanied by an increased number of focal adhesions (Ilic et al., 1995; Ren et al., 2000). One of the biochemical functions of FAK is to activate Rac through p130Cas, Crk,



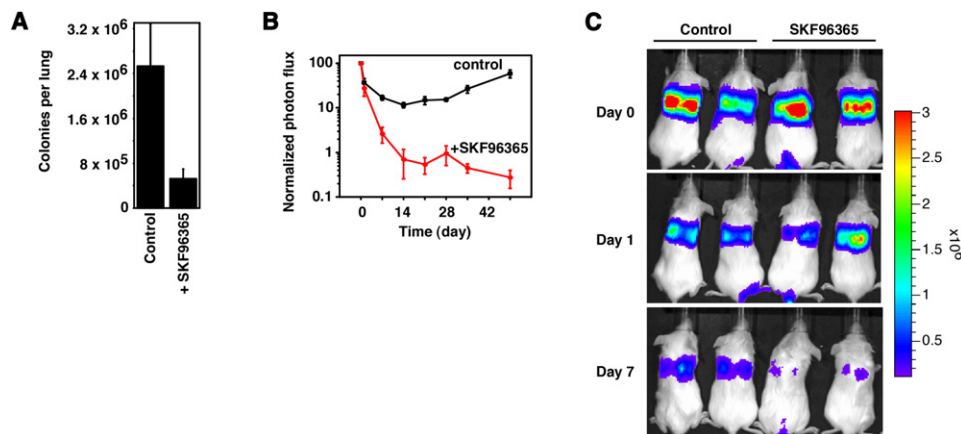


**Figure 7. SKF96365 Inhibits Tumor Metastasis**

(A) Inhibition of 4T1 mouse mammary tumor cell metastasis to the lungs by SKF96365 in a spontaneous metastasis model ( $n = 10$ ).

(B) Inhibition of MDA-MB-231 human breast tumor cell metastasis by SKF96365 in a mouse model.

(C) Representative bioluminescent imaging of mice injected with MDA-MB-231 cells treated without SKF96365 (control,  $n = 7$ ) or with SKF96365 ( $n = 7$ ). The photon flux scale is shown at the right.

Data in (A) and (B) are shown as mean  $\pm$  SEM.

and the DOCK180/ELMO complex (Brugnera et al., 2002). Calpain could cleave talin at adhesion sites, leading to more rapid disassembly rates through additional downstream control of paxillin, vinculin, and zyxin (Franco et al., 2004). Furthermore, other  $\text{Ca}^{2+}$ -sensitive proteins such as myosin light-chain kinase and calcineurin could also mediate the  $\text{Ca}^{2+}$  effect on focal adhesion turnover (Eddy et al., 2000; Lawson and Maxfield, 1995). Moreover, in addition to focal adhesions, podosomes and invadopodia are also adhesion structures, and invadopodia contribute to cancer invasion (Linder, 2007).

Focal adhesion turnover is critical for tumor metastasis. Blocking store-operated  $\text{Ca}^{2+}$  influx slows down focal adhesion turnover, resulting in larger focal adhesions and consequently stronger adherence. Such strong adherence could impede the fast migration of cells, including metastatic cancer cells. Therefore, agents that block store-operated  $\text{Ca}^{2+}$  channels, such as SKF96365, siRNAs for Orai1 and STIM1, or antibodies that specifically block the channel activity of store-operated calcium, are potential therapeutics for tumor metastasis.

## EXPERIMENTAL PROCEDURES

### Cell Lines

MDA-MB-231 cells; GPG29 retrovirus packaging cells; and the TGL reporter construct encoding herpes simplex virus thymidine kinase 1, green fluorescent protein (GFP), and firefly luciferase were gifts from the laboratories of J. Massagué and V. Ponomarev at Memorial Sloan-Kettering Cancer Center. MEFs were derived from day 14 mouse embryos. Cells were grown in high-glucose DMEM with 10% fetal bovine serum. For bioluminescence labeling, MDA-MB-231 cells stably expressing various siRNAs were retrovirally infected with the TGL reporter gene. GFP-positive cells were enriched by fluorescence-activated cell sorting.

### Immunostaining

For immunostaining of nonmigrating cells, cells were plated onto gelatin-coated (for MEFs) or fibronectin-coated (for MDA-MB-231 cells) glass coverslips at  $\sim 20\%$  confluence and allowed to grow overnight. After treatment with or without pharmacological inhibitors (as indicated in the figures) for 2 hr, cells were fixed with 3.7% formaldehyde in PBS for 10 min at room

temperature, permeabilized with 0.1% Triton X-100 in PBS for 3 min, and then blocked with 1% BSA in PBS for 1 hr. Cells were incubated with primary antibody for 1 hr. After washing with PBS, cells were incubated with the appropriate secondary antibody for 1 hr.

Constitutively active G12V mutants of H-Ras or Rac1 were subcloned into pBMN-IRES-GFP retroviral vector. Retroviruses encoding Ras(G12V) or Rac1(G12V) were harvested from the growth medium of GPG29 packaging cells transfected with the respective constructs. MEFs or MDA-MB-231 cells were incubated with retroviruses in growth medium supplemented with 8  $\mu\text{g}/\text{ml}$  polybrene at  $37^\circ\text{C}$  for 3 hr. Cells were further cultured for 48 hr before being used for cell migration or focal adhesion staining.

### Cell Migration and Invasion Assay

Wound-healing and Boyden chamber migration assays were performed as described previously (Guo et al., 2007; McGarrigle et al., 2006; Shan et al., 2006; Yang and Huang, 2005). Matrigel-coated invasion inserts (BD Biosciences) with 8  $\mu\text{m}$  pore membranes were used for invasion assays. For Boyden chamber assay, cells on the inside of the transwell inserts were removed with a cotton swab, and cells on the underside of the inserts were fixed and stained. Photographs of three random fields were taken, and the number of cells was counted to calculate the average number of cells per field that had transmigrated.

### Cell Tracking

MDA-MB-231 cells expressing control siRNA or STIM1 and Orai1 siRNA were cultured in a 35 mm dish overnight. The growth medium was changed to Ringer's solution supplemented with 5% calf serum 2 hr before recording, and cells were maintained at  $37^\circ\text{C}$  throughout the experiment. The random migration of the cells was recorded with a phase contrast microscope, and traces and migration speed of migrating cells were analyzed with MetaMorph.

### Calcium Assay

Calcium assays were performed as described previously (Cvejic et al., 2004; Yang and Huang, 2005). For measurement of store-operated  $\text{Ca}^{2+}$  influx, 3 mM EGTA and 2  $\mu\text{M}$  thapsigargin were added to deplete internal calcium stores.  $\text{Ca}^{2+}$  influx was induced by subsequent addition of 2 mM  $\text{Ca}^{2+}$  (free) after store depletion.

### RNA Interference

The siRNA constructs against human STIM1 and Orai1 were generated using the pSUPER.retro vector according to the manufacturer's instructions (OligoEngine). The sequences used were 5'-GGCTCTGGATACAGTGCTC-3'

for STIM1 and 5'-CGTGCACAATCTCAACTCG-3' for Orai1. siRNA-transfected cells were selected using puromycin and used for  $\text{Ca}^{2+}$  imaging, immunostaining, cell migration, invasion, and metastasis assays. siRNA-resistant mutants for STIM1 and Orai1 were obtained by site-directed mutation of the targeting sequences without changing amino acid sequence (from GGCTCTGGATA CAGTGCTC to GCTCTGGACACTGTGCTC for STIM1 and from CGTGCA CAATCTCAACTCG to CGTGCAACCTGAATTCG for Orai1). The mutants were subcloned into pLNCX2 retroviral vector, and viruses were packaged in GPG29 cells. Rescue experiments were conducted either by infecting siRNA stable cell lines with rescue retrovirus or by coinfecting MDA-MB-231 cells with siRNA retrovirus and rescue retrovirus. STIM1 siRNA results were further confirmed with transient transfection of two pairs of siRNA oligos: 5'-GGAUG CUGUCAUUUUUGATT-3' and 5'-GGGAAGACCUCAUUUACCATT-3'. Orai1 siRNA results were confirmed with stable expression of 5'-TGTCTCTAAGA GAATAAG-3'. For western blots, anti-Orai1 antibody was from NewEast Biosciences and anti-STIM1 antibody was from Santa Cruz Biotechnology.

#### Live-Cell Time-Lapse Recording

MEFs transiently expressing paxillin-GFP were plated on gelatin-coated glass-bottomed 35 mm tissue culture dishes overnight. Cells were maintained at 37°C and pH 7.4 throughout the observation period. Focal adhesion dynamics were quantified according to Webb et al. (2004).

#### MDA-MB-231 Breast Tumor Metastasis in Mice

All animal work was performed in accordance with protocols approved by the Institutional Animal Care and Use Committee of Weill Medical College of Cornell University. NOD/SCID immunodeficient mice were used for experimental lung metastasis experiments. MDA-MB-231 human breast tumor cells expressing the TGL reporter were trypsinized and washed with PBS. This artificial TGL reporter gene encodes a triple fusion protein with herpes simplex virus 1 thymidine kinase fused to the N terminus of enhanced GFP and firefly luciferase fused to the C terminus of GFP (Ponomarev et al., 2004). Subsequently,  $1 \times 10^6$  cells in 0.2 ml PBS were injected into the lateral tail vein. Luciferase-based noninvasive bioluminescent imaging and analysis were performed as described previously (Minn et al., 2005a) with an IVIS Imaging System (Xenogen).

#### 4T1 Mammary Tumor Metastasis in Mice

Female BALB/c mice (6–8 weeks old) were purchased from Charles River. 4T1 tumor cells ( $1 \times 10^6$ ) were injected subcutaneously into the abdominal mammary gland area of mice using 0.1 ml of a single-cell suspension in PBS on day 0. Starting on day 7, when the tumors averaged ~4–5 mm in diameter, SKF96365 or control PBS was administered daily by intraperitoneal injection at 10 mg/kg per mouse until day 25. On day 28, the mice were sacrificed. This dosage regimen was well tolerated with no signs of overt toxicity. Every group included ten mice. Numbers of metastatic 4T1 cells in lungs were determined by clonogenic assay. In brief, lungs were removed from each mouse on day 28, finely minced, and digested in 5 ml of enzyme cocktail containing 1× PBS and 1 mg/ml collagenase type IV for 2 hr at 37°C on a platform rocker. After incubation, samples were filtered through 70  $\mu\text{m}$  nylon cell strainers and washed twice with PBS. Resulting cells were suspended and plated with a series of dilutions in 10 cm tissue culture dishes in RPMI1640 medium containing 60  $\mu\text{M}$  thioguanine for clonogenic growth. Since 4T1 tumor cells are resistant to 6-thioguanine, metastasized tumor cells formed foci after 14 days, at which time they were fixed with methanol and stained with 0.03% methylene blue for counting.

#### Histology

Ten weeks after xenografting, mice were anesthetized and subsequently perfused with PBS and PBS-buffered 4% paraformaldehyde. Lungs were inflated with 1% low-melting agarose, processed for paraffin-embedded sectioning at 8  $\mu\text{m}$ , and stained with H&E. For immunohistochemistry, inflated lungs were embedded in OCT medium and cryosectioned at 10  $\mu\text{m}$ . Cryosections were counterstained with Texas red-conjugated phalloidin and DAPI to reveal actin and nuclei.

#### SUPPLEMENTAL DATA

The Supplemental Data include two movies and can be found with this article online at [http://www.cancer-cell.org/supplemental/S1535-6108\(08\)00438-8](http://www.cancer-cell.org/supplemental/S1535-6108(08)00438-8).

#### ACKNOWLEDGMENTS

We thank D. Webb for the paxillin-GFP plasmid, J. Massagué for MDA-MB-231 cells, V. Ponomarev for the TGL reporter plasmid, G. Gupta for help with bioluminescent imaging, and J. Hou for assistance with histological staining. We are grateful to T. Maack, L. Palmer, M. Zhu, and members of our laboratory for critical reading of the manuscript. This research was supported by the US Department of Defense Breast Cancer Research Program. S.Y. is a recipient of a Postdoctoral Fellowship in Breast Cancer Research from the New York State Department of Health.

Received: March 19, 2008

Revised: August 28, 2008

Accepted: December 29, 2008

Published: February 2, 2009

#### REFERENCES

- Achison, M., Elton, C.M., Hargreaves, P.G., Knight, C.G., Barnes, M.J., and Farn-dale, R.W. (2001). Integrin-independent tyrosine phosphorylation of p125(fak) in human platelets stimulated by collagen. *J. Biol. Chem.* 276, 3167–3174.
- Berridge, M.J., Bootman, M.D., and Roderick, H.L. (2003). Calcium signalling: dynamics, homeostasis and remodelling. *Nat. Rev. Mol. Cell Biol.* 4, 517–529.
- Brugnera, E., Haney, L., Grimsley, C., Lu, M., Walk, S.F., Tosello-Trampont, A.C., Macara, I.G., Madhani, H., Fink, G.R., and Ravichandran, K.S. (2002). Unconventional Rac-GEF activity is mediated through the Dock180-ELMO complex. *Nat. Cell Biol.* 4, 574–582.
- Christofori, G. (2006). New signals from the invasive front. *Nature* 441, 444–450.
- Cvejic, S., Zhu, Z., Felice, S.J., Berman, Y., and Huang, X.Y. (2004). The endogenous ligand Stunted of the GPCR Methuselah extends lifespan in *Drosophila*. *Nat. Cell Biol.* 6, 540–546.
- Dolmetsch, R.E., Xu, K., and Lewis, R.S. (1998). Calcium oscillations increase the efficiency and specificity of gene expression. *Nature* 392, 933–936.
- Dourdin, N., Bhatt, A.K., Dutt, P., Greer, P.A., Arthur, J.S., Elce, J.S., and Huttenlocher, A. (2001). Reduced cell migration and disruption of the actin cytoskeleton in calpain-deficient embryonic fibroblasts. *J. Biol. Chem.* 276, 48382–48388.
- Eddy, R.J., Pierini, L.M., Matsumura, F., and Maxfield, F.R. (2000).  $\text{Ca}^{2+}$ -dependent myosin II activation is required for uropod retraction during neutrophil migration. *J. Cell Sci.* 113, 1287–1298.
- Fanger, C.M., Hoth, M., Crabtree, G.R., and Lewis, R.S. (1995). Characterization of T cell mutants with defects in capacitative calcium entry: genetic evidence for the physiological roles of CRAC channels. *J. Cell Biol.* 131, 655–667.
- Feske, S., Prakriya, M., Rao, A., and Lewis, R.S. (2005). A severe defect in CRAC  $\text{Ca}^{2+}$  channel activation and altered  $\text{K}^{+}$  channel gating in T cells from immunodeficient patients. *J. Exp. Med.* 202, 651–662.
- Feske, S., Gwack, Y., Prakriya, M., Srikanth, S., Puppel, S.H., Tanasa, B., Hogan, P.G., Lewis, R.S., Daly, M., and Rao, A. (2006). A mutation in Orai1 causes immune deficiency by abrogating CRAC channel function. *Nature* 441, 179–185.
- Fidler, I.J. (2003). The pathogenesis of cancer metastasis: the 'seed and soil' hypothesis revisited. *Nat. Rev. Cancer* 3, 453–458.
- Franco, S.J., Rodgers, M.A., Perrin, B.J., Han, J., Bennin, D.A., Critchley, D.R., and Huttenlocher, A. (2004). Calpain-mediated proteolysis of talin regulates adhesion dynamics. *Nat. Cell Biol.* 6, 977–983.
- Guo, D., Tan, Y.C., Wang, D., Madhusoodanan, K.S., Zheng, Y., Maack, T., Zhang, J.J., and Huang, X.Y. (2007). A Rac-cGMP signaling pathway. *Cell* 128, 341–355.
- Guo, W., and Giancotti, F.G. (2004). Integrin signalling during tumour progression. *Nat. Rev. Mol. Cell Biol.* 5, 816–826.
- Hanahan, D., and Weinberg, R.A. (2000). The hallmarks of cancer. *Cell* 100, 57–70.
- Huttenlocher, A., Palecek, S.P., Lu, Q., Zhang, W., Mellgren, R.L., Lauffenburger, D.A., Ginsberg, M.H., and Horwitz, A.F. (1997). Regulation of cell migration by the calcium-dependent protease calpain. *J. Biol. Chem.* 272, 32719–32722.

- Ilic, D., Furuta, Y., Kanazawa, S., Takeda, N., Sobue, K., Nakatsuji, N., Nomura, S., Fujimoto, J., Okada, M., and Yamamoto, T. (1995). Reduced cell motility and enhanced focal adhesion contact formation in cells from FAK-deficient mice. *Nature* 377, 539–544.
- Komuro, H., and Rakic, P. (1993). Modulation of neuronal migration by NMDA receptors. *Science* 260, 95–97.
- Lawson, M.A., and Maxfield, F.R. (1995).  $\text{Ca}^{2+}$ - and calcineurin-dependent recycling of an integrin to the front of migrating neutrophils. *Nature* 377, 75–79.
- Lee, J., Ishihara, A., Oxford, G., Johnson, B., and Jacobson, K. (1999). Regulation of cell movement is mediated by stretch-activated calcium channels. *Nature* 400, 382–386.
- Lewis, R.S. (2001). Calcium signaling mechanisms in T lymphocytes. *Annu. Rev. Immunol.* 19, 497–521.
- Lewis, R.S. (2007). The molecular choreography of a store-operated calcium channel. *Nature* 446, 284–287.
- Linder, S. (2007). The matrix corroded: podosomes and invadopodia in extracellular matrix degradation. *Trends Cell Biol.* 17, 107–117.
- Liou, J., Kim, M.L., Heo, W.D., Jones, J.T., Myers, J.W., Ferrell, J.E., Jr., and Meyer, T. (2005). STIM is a  $\text{Ca}^{2+}$  sensor essential for  $\text{Ca}^{2+}$ -store-depletion-triggered  $\text{Ca}^{2+}$  influx. *Curr. Biol.* 15, 1235–1241.
- Mareel, M., and Leroy, A. (2003). Clinical, cellular, and molecular aspects of cancer invasion. *Physiol. Rev.* 83, 337–376.
- Marks, P.W., and Maxfield, F.R. (1990). Transient increases in cytosolic free calcium appear to be required for the migration of adherent human neutrophils. *J. Cell Biol.* 110, 43–52.
- McGarrigle, D., Shan, D., Yang, S., and Huang, X.Y. (2006). Role of tyrosine kinase Csk in G protein-coupled receptor- and receptor tyrosine kinase-induced fibroblast cell migration. *J. Biol. Chem.* 281, 10583–10588.
- Mercer, J.C., Dehaven, W.I., Smyth, J.T., Wedel, B., Boyles, R.R., Bird, G.S., and Putney, J.W., Jr. (2006). Large store-operated calcium selective currents due to co-expression of Orai1 or Orai2 with the intracellular calcium sensor, Stim1. *J. Biol. Chem.* 281, 24979–24990.
- Minn, A.J., Gupta, G.P., Siegel, P.M., Bos, P.D., Shu, W., Giri, D.D., Viale, A., Olshen, A.B., Gerald, W.L., and Massagué, J. (2005a). Genes that mediate breast cancer metastasis to lung. *Nature* 436, 518–524.
- Minn, A.J., Kang, Y., Serganova, I., Gupta, G.P., Giri, D.D., Doubrovina, M., Ponomarev, V., Gerald, W.L., Blasberg, R., and Massagué, J. (2005b). Distinct organ-specific metastatic potential of individual breast cancer cells and primary tumors. *J. Clin. Invest.* 115, 44–55.
- Mogami, H., Nakano, K., Tepikin, A.V., and Petersen, O.H. (1997).  $\text{Ca}^{2+}$  flow via tunnels in polarized cells: recharging of apical  $\text{Ca}^{2+}$  stores by focal  $\text{Ca}^{2+}$  entry through basal membrane patch. *Cell* 88, 49–55.
- Nishiyama, M., Hoshino, A., Tsai, L., Henley, J.R., Goshima, Y., Tessier-Lavigne, M., Poo, M.M., and Hong, K. (2003). Cyclic AMP/GMP-dependent modulation of  $\text{Ca}^{2+}$  channels sets the polarity of nerve growth-cone turning. *Nature* 423, 990–995.
- Parekh, A.B., and Penner, R. (1997). Store depletion and calcium influx. *Physiol. Rev.* 77, 901–930.
- Peinelt, C., Vig, M., Koomoa, D.L., Beck, A., Nadler, M.J., Koblan-Huberson, M., Lis, A., Fleig, A., Penner, R., and Kinet, J.P. (2006). Amplification of CRAC current by STIM1 and CRACM1 (Orai1). *Nat. Cell Biol.* 8, 771–773.
- Pettit, E.J., and Fay, F.S. (1998). Cytosolic free calcium and the cytoskeleton in the control of leukocyte chemotaxis. *Physiol. Rev.* 78, 949–967.
- Ponomarev, V., Doubrovina, M., Serganova, I., Vider, J., Shavrin, A., Beresten, T., Ivanova, A., Ageyeva, L., Tourkova, V., Balatoni, J., et al. (2004). A novel triple-modality reporter gene for whole-body fluorescent, bioluminescent, and nuclear noninvasive imaging. *Eur. J. Nucl. Med. Mol. Imaging* 31, 740–751.
- Prakriya, M., Feske, S., Gwack, Y., Srikanth, S., Rao, A., and Hogan, P.G. (2006). Orai1 is an essential pore subunit of the CRAC channel. *Nature* 443, 230–233.
- Pulaski, B.A., and Ostrand-Rosenberg, S. (1998). Reduction of established spontaneous mammary carcinoma metastases following immunotherapy with major histocompatibility complex class II and B7.1 cell-based tumor vaccines. *Cancer Res.* 58, 1486–1493.
- Ren, X.D., Kiessens, W.B., Sieg, D.J., Otey, C.A., Schlaepfer, D.D., and Schwartz, M.A. (2000). Focal adhesion kinase suppresses Rho activity to promote focal adhesion turnover. *J. Cell Sci.* 113, 3673–3678.
- Ridley, A.J., and Hall, A. (1992). The small GTP-binding protein rho regulates the assembly of focal adhesions and actin stress fibers in response to growth factors. *Cell* 70, 389–399.
- Ridley, A.J., Schwartz, M.A., Burridge, K., Firtel, R.A., Ginsberg, M.H., Borisy, G., Parsons, J.T., and Horwitz, A.R. (2003). Cell migration: integrating signals from front to back. *Science* 302, 1704–1709.
- Roos, J., DiGregorio, P.J., Yeromin, A.V., Ohlsen, K., Lioudyno, M., Zhang, S., Safrina, O., Kozak, J.A., Wagner, S.L., Cahalan, M.D., et al. (2005). STIM1, an essential and conserved component of store-operated  $\text{Ca}^{2+}$  channel function. *J. Cell Biol.* 169, 435–445.
- Schlaepfer, D.D., and Hunter, T. (1998). Integrin signalling and tyrosine phosphorylation: just the FAKs? *Trends Cell Biol.* 8, 151–157.
- Shan, D., Chen, L., Njardarson, J.T., Gaul, C., Ma, X., Danishefsky, S.J., and Huang, X.Y. (2005). Synthetic analogues of migrastatin that inhibit mammary tumor metastasis in mice. *Proc. Natl. Acad. Sci. USA* 102, 3772–3776.
- Shan, D., Chen, L., Wang, D., Tan, Y.C., Gu, J.L., and Huang, X.Y. (2006). The g protein  $\alpha_{13}$  is required for growth factor-induced cell migration. *Dev. Cell* 10, 707–718.
- Siciliano, J.C., Toutant, M., Derkinderen, P., Sasaki, T., and Girault, J.A. (1996). Differential regulation of proline-rich tyrosine kinase 2/cell adhesion kinase beta (PYK2/CAKbeta) and pp125(FAK) by glutamate and depolarization in rat hippocampus. *J. Biol. Chem.* 271, 28942–28946.
- Sjoberg, T., Jones, S., Wood, L.D., Parsons, D.W., Lin, J., Barber, T.D., Mandelker, D., Leary, R.J., Ptak, J., Silliman, N., et al. (2006). The consensus coding sequences of human breast and colorectal cancers. *Science* 314, 268–274.
- Soboloff, J., Spassova, M.A., Tang, X.D., Hewavitharana, T., Xu, W., and Gill, D.L. (2006). Orai1 and STIM1 reconstitute store-operated calcium channel function. *J. Biol. Chem.* 281, 20661–20665.
- Steeg, P.S. (2006). Tumor metastasis: mechanistic insights and clinical challenges. *Nat. Med.* 12, 895–904.
- Vig, M., Peinelt, C., Beck, A., Koomoa, D.L., Rabah, D., Koblan-Huberson, M., Kraft, S., Turner, H., Fleig, A., Penner, R., and Kinet, J.P. (2006). CRACM1 is a plasma membrane protein essential for store-operated  $\text{Ca}^{2+}$  entry. *Science* 312, 1220–1223.
- Wang, D., Tan, Y.C., Kreitzer, G.E., Nakai, Y., Shan, D., Zheng, Y., and Huang, X.Y. (2006). G proteins G12 and G13 control the dynamic turnover of growth factor-induced dorsal ruffles. *J. Biol. Chem.* 281, 32660–32667.
- Webb, D.J., Parsons, J.T., and Horwitz, A.F. (2002). Adhesion assembly, disassembly and turnover in migrating cells—over and over and over again. *Nat. Cell Biol.* 4, E97–E100.
- Webb, D.J., Donais, K., Whitmore, L.A., Thomas, S.M., Turner, C.E., Parsons, J.T., and Horwitz, A.F. (2004). FAK-Src signalling through paxillin, ERK and MLCK regulates adhesion disassembly. *Nat. Cell Biol.* 6, 154–161.
- Weiss, L. (2000). Metastasis of cancer: a conceptual history from antiquity to the 1990s. *Cancer Metastasis Rev.* 19, I–XI, 193–383.
- Yang, S., and Huang, X.Y. (2005).  $\text{Ca}^{2+}$  influx through L-type  $\text{Ca}^{2+}$  channels controls the trailing tail contraction in growth factor-induced fibroblast cell migration. *J. Biol. Chem.* 280, 27130–27137.
- Yeromin, A.V., Zhang, S.L., Jiang, W., Yu, Y., Safrina, O., and Cahalan, M.D. (2006). Molecular identification of the CRAC channel by altered ion selectivity in a mutant of Orai. *Nature* 443, 226–229.
- Yoo, A.S., Cheng, I., Chung, S., Grenfell, T.Z., Lee, H., Pack-Chung, E., Handler, M., Shen, J., Xia, W., Tesco, G., et al. (2000). Presenilin-mediated modulation of capacitative calcium entry. *Neuron* 27, 561–572.
- Zhang, S.L., Yeromin, A.V., Zhang, X.H., Yu, Y., Safrina, O., Penna, A., Roos, J., Stauderman, K.A., and Cahalan, M.D. (2006). Genome-wide RNAi screen of  $\text{Ca}^{2+}$  influx identifies genes that regulate  $\text{Ca}^{2+}$  release-activated  $\text{Ca}^{2+}$  channel activity. *Proc. Natl. Acad. Sci. USA* 103, 9357–9362.